Transport Coefficients of Xylene Isomers

Bernard Rousseau[†] and Janka Petravic*

Research School of Chemistry, Australian National University, Canberra, ACT 0200, Australia

Received: February 7, 2002; In Final Form: September 19, 2002

We have investigated the effects of pressure and temperature on viscosity and self-diffusion coefficients of the *o*- (OX), *m*- (MX), and *p*-xylene (PX) isomers in the temperature and pressure range of 298−348 K and 0.1−100 MPa, respectively. The transport coefficients have been computed using equilibrium molecular dynamics and the Green−Kubo formalism. The xylene isomers are described as multisite rigid molecules interacting with the OPLS force field. Computed densities and viscosities are in good agreement with experimental data and a correlation based on the rough hard-sphere theory. For each studied state point, the OPLS model is able to reproduce the relative order of densities and viscosities of the isomers. Using both sets of computed viscosity and self-diffusion data, we show that for xylene isomers the Stokes−Einstein (SE) relation is valid at the molecular level. Effective hydrodynamic diameters of isomers obtained from SE relationship are noticeably different. Finally, we discuss the influence of electrostatic interactions and mass distribution on transport properties and on the SE effective hydrodynamic diameter.

1. Introduction

Knowledge of transport properties of multicomponent gases and oils is of great economical importance in reservoir modeling, planning of transport, and design of industrial plants. Unfortunately, these mixtures consist of a variety of compound types, and it is impossible to get the detailed fluid composition. A usual way to treat the problem is to represent the fluid by some selected model compounds, chosen as representative of the most important chemical species in the fluid. The system is then reduced to a much smaller and tractable set of molecules whose mixture is a model of the unknown fluid. Xylene isomers are present in crude oils, and they represent a typical case of substituted aromatics. Therefore, the knowledge of their properties is required to predict the properties of mixtures containing aromatics.

Molecular simulation is becoming a standard tool for the computation of a range of liquid properties relevant to the oil industry. Although many studies have been devoted to the study of transport properties of linear and branched alkanes or alkane mixtures, much less has been done on aromatics. As an example, transport properties of xylene isomers have never, to our knowledge, been evaluated by computer simulation. This may be due to the fact that OX and MX have a small dipole moment which requires the computation of time-consuming long-range interactions compared to alkanes. In the following, we evaluate the ability of the OPLS force field from Jorgensen[1] to predict the viscosity of xylene isomers in a large range of temperatures and pressures. This potential has been developed for use in computer simulations of equilibrium and structural properties of substituted benzenes but, to our knowledge, has not yet been tested against transport properties. The predictive power of molecular simulation relies on the ability of effective force fields to reproduce other properties at other state points. As xylene isomers (at the same P and T) have very close shear viscosity (especially MX and PX), we believe this work is a rigorous test of the ability of the force field to predict transport coefficient. Also, it can be seen from the available experimental data that the order of viscosities for isomers at a given P and T does not follow the order of densities. Therefore, we want to test whether the OPLS potential is able to reproduce this peculiar behavior and how much quantitative agreement it can give. We also want to see whether the order of the self-diffusion coefficients would be like opposite densities or opposite viscosities.

The paper is organized as follows: first, we describe the OPLS model and the simulation details. Then, we present the molecular simulation results for density, viscosity, and self-diffusion. Viscosity and density data are compared with available experimental data and a correlation from Assael. Finally, we discuss the results in the framework of the Stokes−Einstein (SE) relation. We focus here on the effect of electrostatic interactions and mass distribution on transport properties and on the SE effective hydrodynamic diameter.

2. Model and Simulation Details

To our knowledge, there has been no force field specifically designed for xylene isomers. Therefore, we used the parameters from the OPLS set for pure liquid substituted benzenes, proposed by Jorgensen and Nguyen.[1] This potential had been obtained by merging of the Lennard-Jones (LJ) parameters σ and ϵ and partial charges q of an all-atom model of benzene[2] and LJ parameters for the substituent from some other OPLS set. The charge on the substituent is equal to the partial charge on the substituted hydrogen. The OPLS parameters used in this work are given in Table 1.

It had been shown that purely LJ six-site models for aromatics do not give the correct viscosity without the added electrostatic interaction to represent the electron density of the π-cloud electrons.[3] The partial charges on hydrogens and carbons in benzene in ref 2 are based on ab initio estimates from ref 4 and therefore take into account this effect. They were subsequently optimized to yield the correct thermophysical properties of liquid benzene.

* Corresponding author: e-mail janka@rsc.anu.edu.au.
[†] Permanent address: Laboratoire de Chimie Physique, Bâtiment 349, Université Paris-Sud, 91405 Orsay, France. E-mail: rousseau@lcp.u-psud.fr.

10.1021/jp025605r CCC: $22.00
Published on Web 11/12/2002

TABLE 1: OPLS Potential Parameters and Bond Lengths for Substituted Benzenes. See Text for Definitions

	potential parameters		
atom or united atom	σ [Å]	ϵ [kJ mol^{-1}]	q [e]
C	3.55	0.293	−0.115
H	2.42	0.125	+0.115
CH_3	3.80	0.711	+0.115
bond lengths			
C−C		1.40 Å	
C−H		1.08 Å	
C−CH_3		1.51 Å	

The united-atom methyl group in toluene corresponds to methyl situated on the site adjacent to nitrogen in amides and peptides.[5] These LJ parameters were shown in later work to give correct densities and heats of vaporization if used for sites adjacent to sulfur in compounds such as thiols and alkyl sulfides[6] and in alkyl ethers on the sites adjacent to oxygen.[7]

The merged potential for substituted benzenes was subsequently used to show that density and specific heat, at ambient temperature and pressure, were correctly reproduced for toluene.[8] From this, the authors in ref 8 drew the conclusion that the transferability of the LJ parameters from aliphatic to aromatic systems is not problematic and the use of merged charges is viable. This general conclusion, although based on simulation results, may be too far-fetched, since merging of charges and LJ potentials from different sources without reoptimization is dangerous. For example, parameters characterizing dispersion interactions are not independent of dipole moment in polar molecules, including aromatics. In this work we test whether this potential can reproduce density and viscosity of xylenes.

The Lennard-Jones potential U_{ij}^{LJ} between two sites i and j at distance r is

$$U_{ij}^{LJ}(r) = 4\epsilon_{ij}[(\sigma_{ij}/r)^{12} - (\sigma_{ij}/r)^{6}] \quad (1)$$

where the combination rules for the LJ parameters ϵ_{ij} and σ_{ij} are

$$\epsilon_{ij} = (\epsilon_i\epsilon_j)^{1/2} \quad \text{and} \quad \sigma_{ij} = (\sigma_i\sigma_j)^{1/2} \quad (2)$$

and only the sites on different molecules interact. The LJ interactions were truncated at $r_c = 2.5\sigma_{CH_3}$. Beyond the cutoff, the long-range corrections to potential energy and hydrostatic pressure were included in order to account for the truncation effects.[9]

Electrostatic interactions were treated using the Ewald summation technique. The pressure tensor was evaluated using the molecular representation of Nosé and Klein.[10] In our simulations, the real space electrostatic interactions were always cut off at half the box length, $L/2$, the reciprocal space wavevector cutoff was at $k_{max} = 6(2\pi/L)$, and the convergence acceleration factor was chosen as $\kappa = 1.8\pi/L$. These parameters were used even with constant-pressure simulations. This keeps the relative errors due to cutoff in distance and wavevector constant, which was sufficient since the fluctuations of L during *NPT* simulations are not very large.

There are two possible approaches to computation of shear viscosity in equilibrium.[11] One involves equilibrium molecular dynamics (EMD) simulation of a system and calculation of shear viscosity from the stress−stress autocorrelation functions (Green−Kubo relations). In the other, nonequilibrium molecular dynamics (NEMD) approach, homogeneous shear is explicitly included in the equations of motion in order to create the response flux equal to the shear stress appearing in the Green−Kubo relations. Viscous heating is removed using some thermostating mechanism, and the steady-state shear viscosity is calculated directly from the constitutive relation as a function of strain rate. For low strain rates, in the "Newtonian regime" viscosity is independent of strain rate and equal to the Green−Kubo value. If this "plateau" occurs only for strain rates too low to be computationally accessible, zero shear viscosity is obtained by extrapolation and is still in very good agreement with the value obtained by EMD. In this study, we chose to use the EMD approach. One reason for this choice was that it allowed us to compute both the diffusion coefficient and shear viscosity in the same run.

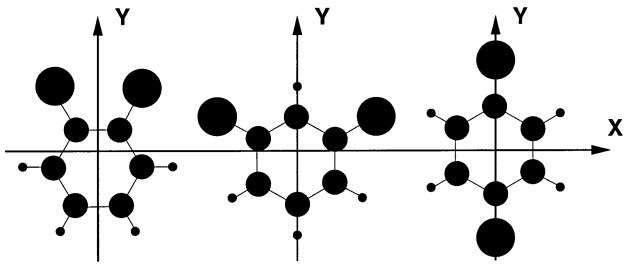

Figure 1. Principal axes of rotation for xylene isomers.

TABLE 2: Moments of Inertia (in kg mol^{-1} Å^2) of Xylene Isomers in the System of Principal Axes[a]

isomer	I_{xx}	I_{yy}	I_{zz}
OX	0.2223	0.1494	0.3717
MX	0.1335	0.2703	0.4038
PX	0.3308	0.0890	0.4270

[a] $I_{zz} = I_{xx} + I_{yy}$ reflects the fact that the molecules are planar.

Equilibrium molecular dynamics simulations were performed on systems consisting of $N = 128$ molecules per periodic cell. The molecules were treated as rigid bodies, with separate equations of motion for the center-of-mass translation and the rotation. The translational equations of motion included temperature and pressure control. The center-of-mass translational temperature T_{CM} was fixed using the Gauss thermostat. In the *NPT* simulations, the pressure of the system was controlled with the Nosé−Hoover integral feedback, and the coefficient Q was chosen as $Q = 50/Nk_BT$ in all simulations.

Because of the large cutoff radius and the large size of xylene molecules relative to the size of the periodic cell, it can sometimes happen that a site is inside the minimum image cell, while its center of mass is not. In this case, care has to be taken when employing the minimum image convention in combination with the molecular form of the pressure tensor. For the purpose of calculation of the elements of the pressure tensor, it is important not to move the center of mass back into the minimum image cell, because this gives the wrong center-of-mass distance corresponding to the intermolecular force.

Rotations were described with use of quaternions.[12] A sketch of positions of the principal axes of rotation for different isomers is presented in Figure 1, and their moments of inertia are given in Table 2. The moments I_{xx} and I_{yy} refer to rotations about the principal axes in the molecular plane, and $I_{zz} = I_{xx} + I_{yy}$ reflects the fact that the molecules are planar.

The set of first-order equations of motion was integrated using five valued Gear predictor−corrector algorithm, with a time step of 4 fs.

The initial distributions for different state points were prepared at a low density and the desired translational temperature. After that, the system was equilibrated for 250 000 time steps at a

specified pressure and temperature using the Nosé−Hoover integral feedback in order to bring the pressure to the desired value while keeping the translational center-of-mass temperature constant with the Gauss thermostat. The system was considered in equilibrium when the translational and rotational temperatures became equal and the off-diagonal elements of the pressure tensor were close to zero. An additional 200 000 time steps of *NPT* simulations were then performed in order to determine the densities of the system at chosen state points. Each system was subsequently equilibrated in the *NVT* ensemble at the density obtained for the considered state point. The final configuration was used to calculate transport coefficients according to the Green−Kubo formalism. The calculation of diffusion coefficients has much greater accuracy than the calculation of viscosity, because it is a one-particle property. Therefore, it requires much shorter runs. Diffusion coefficients were calculated together with viscosities during 200 000 time steps, and additional runs of 2 million time steps in total were used for calculations of viscosity, since simultaneous calculations of both slow down the computation. The length of the shift register in the calculation of the diffusion coefficient was 25 ps, and in the calculation of viscosity it was set to 50 ps because it was observed that the stress autocorrelation function has a longer tail. Viscosity runs were split into eight runs of equal length in order to estimate the statistical spread of the results, whereas the error in the diffusion coefficient was estimated from the results of two independent runs of 100 000 time steps.

3. Prediction of Transport Coefficients

3.1 Viscosity. In this section, we compare viscosities obtained from molecular simulation with experimental values. Our simulation results are compared with two independent sets of data: a correlation from Assael and Dymond (AS) and experimental data from Et-Tahir (ET). Assael et al.[13] have proposed a correlation for aromatic hydrocarbons which covers a temperature range of roughly 290−350 K and pressure up to 100 MPa. This correlation is based on considerations of hard-sphere theory and uses viscosity data from Kashiwagi et al.,[14] Dymond et al.,[15] and Assael et al.[16] The accuracy of viscosity predictions using this correlation is estimated to be better than 5%.

We also used an independent set of data from Et-Tahir[17] including viscosity data in the temperature range 293−363 K and pressure up to 100 MPa. Although Et-Tahir experiments were done at constant temperature and pressure, the density was required in order to interpret their viscosity measurements. They measured density along several isotherms using a vibrating cell in a range of pressure up to 40 MPa. Densities at pressure up to 100 MPa were extrapolated from data in the range 0.1−40 MPa using a modified Tait equation of the form

$$\frac{1}{\rho(T,P)} = \frac{1}{\rho_0(T)} - A(T)\ln\left[1 + \frac{P-1}{B(T)}\right] \qquad (3)$$

where $A(T)$ and $B(T)$ are the adjustable parameters derived for each isotherm and $\rho_0(T)$ is some reference density chosen at the pressure of 0.1 MPa. Most of Et-Tahir's work was done at different temperatures than those previously published and used in our MD simulations. Therefore, a linear fit was done on each isobaric set of experimental data to interpolate densities and viscosities at temperatures used in this work. The overall accuracy for the experimental data from Et-Tahir is of the order of 0.5% for densities and 2% for viscosities.

TABLE 3: Densities ρ for Xylenes at Five State Points and Deviations Δ between Different Sets of Data in Percent[a]

state variables		ρ [kg m^{-3}]			Δ [%]		
P [MPa]	T [K]	MD	AS	ET[b]	MD/AS[c]	MD/ET	ET/AS
				o-Xylene			
0.1	323.0	853.1	854.9	852.9 (i)	0.22	−0.02	0.24
40.0	323.0	882.5	882.4	880.4 (i)	−0.01	−0.24	0.23
100.0	323.0	914.3	912.9	909.6 (e)	−0.15	−0.52	0.37
0.1	298.0	875.8	876.5	874.0	0.08	−0.21	0.29
0.1	348.0	828.6	833.3	831.9 (i)	0.56	0.40	0.17
				m-Xylene			
0.1	323.0	835.7	839.4	837.1 (i)	0.45	0.17	0.28
40.0	323.0	865.4	869.9	866.1 (i)	0.52	0.08	0.44
100.0	323.0	898.6	902.8	899.9 (e)	0.46	0.14	0.32
0.1	298.0	858.0	860.1	858.8	0.24	0.09	0.15
0.1	348.0	810.9	817.6	815.4 (i)	0.83	0.55	0.28
				p-Xylene			
0.1	323.0	831.5	834.9	833.7 (i)	0.41	0.26	0.15
40.0	323.0	862.1	865.3	863.0 (i)	0.37	0.10	0.27
100.0	323.0	895.7	898.1	891.6 (e)	0.26	−0.46	0.72
0.1	298.0	854.0	855.8	854.9	0.21	0.11	0.11
0.1	348.0	807.3	812.9	812.6 (i)	0.69	0.65	0.04
av dev					0.36	0.27	0.27

[a] MD = molecular dynamics simulations in (NPT); AS = Assael correlation; ET = Et-Tahir experimental data. [b] (i) Interpolated from data at different temperatures. (e) Extrapolated from data at lower pressure (see ref 17). [c] MD/AS is the deviation between MD and AS, relative to AS. Statistical uncertainty of the simulation results is less than 0.1%.

Five state points have been selected in order to investigate temperature and pressure effects on viscosity. The temperature range extends from 298 to 348 K, and the pressure range is from 0.1 to 100 MPa. Before computing transport coefficients, we tested the ability of the potential to reproduce the fluid density over our defined range of pressure and temperature. It is important to recall here that the OPLS potential has been derived to reproduce bulk fluid properties at atmospheric pressure and temperature. Moreover, the parameter set for substituted hydrocarbons was built by merging together the parameters for benzene and ethers. Therefore, it was not expected to be very accurate in a large range of state points. Table 3 shows the densities obtained from molecular simulations in the (NPT) ensemble for the five studied state points along with the Et-Tahir experimental data and Assael correlation results. The statistical error from MD simulations, computed on eight independent blocks of data, is smaller than 0.1%. First of all, we notice that the deviation between correlation from Assael and data from Et-Tahir is less than 0.3% and that the largest deviations are observed with values at high pressure, i.e., where Et-Tahir data have been extrapolated. However, this agreement is quite satisfactory. The agreement of MD results with AS and ET is also very good: the average relative deviation from AS correlation and ET data is less than 0.4% and 0.3%, respectively, which is of the same order of magnitude as the deviations between AS and ET data. The general tendency of the OPLS potential is to slightly underestimate the densities except for OX. The largest deviations are observed at atmospheric pressure and high temperature but never exceed 0.83%. There might be a trend that the agreement worsens slightly at elevated temperatures. This would agree with the results for benzene by Wick et al.,[18] who found good agreement for the saturated liquid densities at 300 K but systematically lower saturated densities at elevated temperatures and a critical temperature 25 K below its experimental counterpart. Therefore, we can consider that the volumetric properties in this temper-

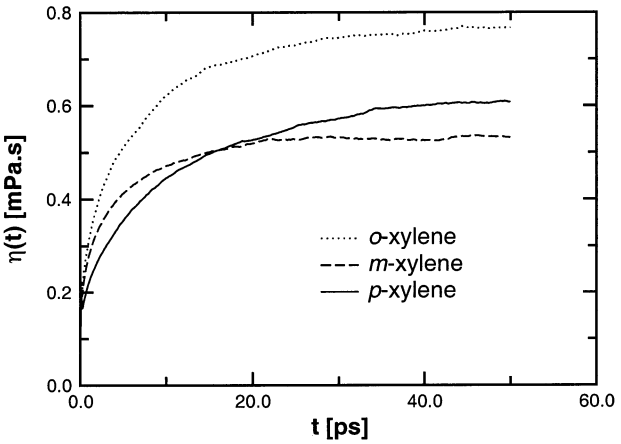

Figure 2. Integrals of the symmetrized traceless stress tensor autocorrelation function for OX, MX, and PX at $T = 298$ K and $P = 0.1$ MPa.

TABLE 4: Viscosities for Xylenes at Five State Points and Deviations between Different Sets of Data in Percent

state variables		η [mPa s]			Δ [%]		
P [MPa]	T [K]	MD	AS	ET[b]	MD/AS[c]	MD/ET	ET/AS
				o-Xylene			
0.1	323.0	0.535	0.560	0.562 (i)	4.5	4.8	−0.4
40.0	323.0	0.820	0.756	0.793 (i)	−2.7	−3.4	−4.9
100.0	323.0	1.200	1.104	1.165 (e)	−8.7	−3.0	−5.5
0.1	298.0	0.767	0.751	0.758	−2.1	−1.2	−0.9
0.1	348.0	0.458	0.445	0.432 (i)	−2.9	−6.0	2.9
				m-Xylene			
0.1	323.0	0.420	0.434	0.448 (i)	3.2	6.3	−3.2
40.0	323.0	0.592	0.594	0.597 (i)	0.3	0.8	−0.5
100.0	323.0	0.870	0.876	0.853 (e)	0.7	−2.0	2.6
0.1	298.0	0.532	0.562	0.580	5.3	8.3	−3.2
0.1	348.0	0.335	0.350	0.354 (i)	4.3	5.4	1.2
				p-Xylene			
0.1	323.0.0	0.467	0.452	0.472 (i)	−3.3	1.1	−4.4
40.0	323.0	0.599	0.615	0.618 (i)	2.6	3.1	−0.5
100.0	323.0	0.920	0.898	0.909 (e)	−2.4	−1.2	−1.2
0.1	298.0	0.609	0.584	0.619	4.3	1.6	−6.0
0.1	348.0	0.385	0.366	0.367 (i)	−5.2	−4.9	−0.3
av dev			3.5	3.5	2.5		

[a] MD = molecular dynamics simulations in (NPT); AS = Assael correlation; ET = Et-Tahir experimental data. [b] (i) Interpolated from data at different temperatures. (e) Extrapolated from data at lower pressure (see ref 17). [c] MD/AS is the deviation between MD and AS, relative to AS. Average statistical uncertainty of the simulation results is 5%.

ature and pressure range are well reproduced by the OPLS potential and that no further refinement of the parameters is necessary.

In Figure 2, we show the integrals of the symmetrized traceless stress tensor[19] autocorrelation functions vs time for OX, MX, and PX at $T = 298$ K and $P = 0.1$ MPa. The shear viscosity is given by the infinite time integral of the correlation function. For all systems studied here, the average value of the viscosity was computed from the time integral of the correlation function at the time of 50 ps. It was found that the correlation time was the shortest for MX and the longest for PX, while OX had the largest noise, probably due to the lowest symmetry of the mass distribution. All the correlation functions (especially for *o*- and *p*-xylene) have very long tails. We chose the time window of 50 ps as a compromise between the time needed in order for the correlation functions to reach a plateau and the time after which the integrals became too noisy. Better estimates for the plateau and lower noise levels for longer time windows

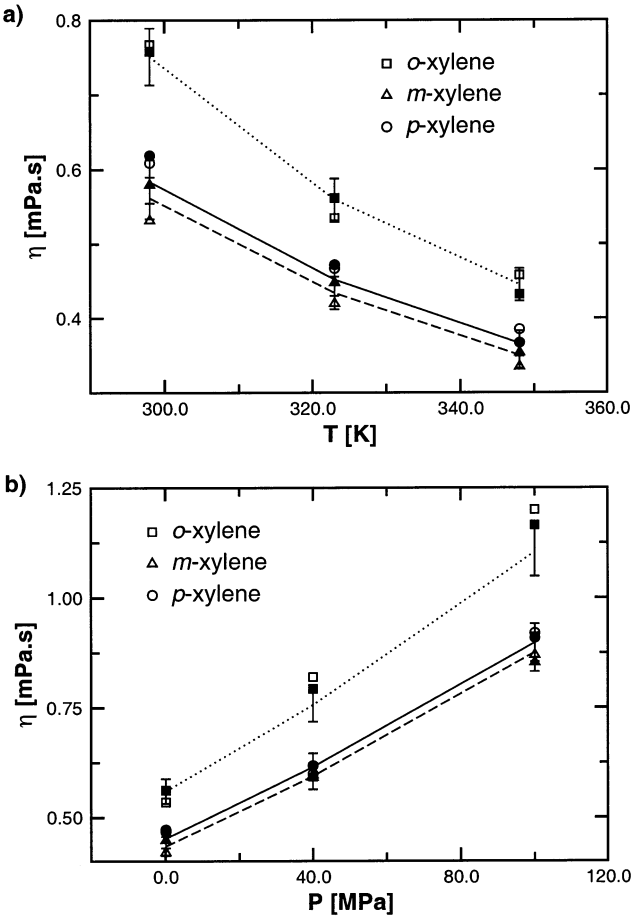

Figure 3. Dependence of viscosity on (a) temperature and (b) pressure from simulation (open symbols), Assael correlations (OX, dotted line; MX, dashed line; PX, full line), and Et-Tahir experiments (full symbols).

could not be achieved for the total length of our runs (10 ns). The corresponding effect with NEMD would be that the Newtonian limit is reached only for the strain rates lower than 0.01 ps^{-1}, which is at the limit of accessibility by computer simulation.

Viscosity data are presented in Table 4 along with data from AS and ET. The same data are compared in Figure 3. The average statistical uncertainty of the simulation results is 5%. The typical behavior for fluid viscosity as a function of T and P is correctly reproduced. The agreement between MD and both reference sets is good: The average deviation for all studied states is less than 4%. The largest deviations are observed for OX and PX at the highest P and T but never exceed 9%. Therefore, we conclude that the OPLS potential is accurate enough for viscosity prediction in the range of T and P explored here.

3.2. Diffusion. Given the good agreement of the simulation results using the OPLS force field with the experimental densities and viscosities, we assume that the same potential can be used to estimate the diffusion coefficient with a similar degree of accuracy. To our knowledge, there are no published experimental or simulation results of diffusion coefficients for xylene isomers, and this work is a first attempt to produce such data.

The representative velocity autocorrelation function integrals at $T = 298$ K and $P = 0.1$ MPa are shown in Figure 4, and the trends with the change of temperature and pressure are shown in Figure 5. The values of the diffusion coefficient obtained at five investigated state points are presented in Table 5.

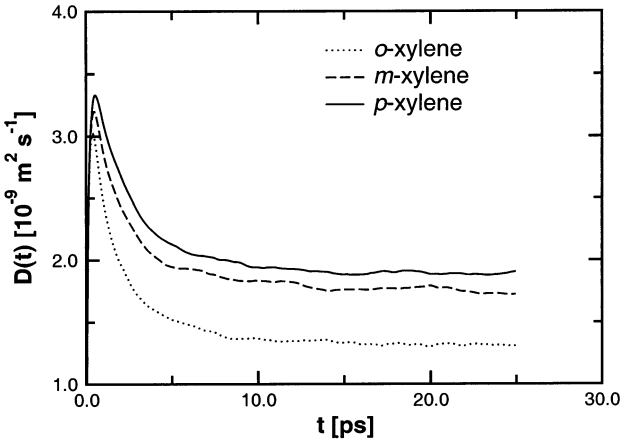

Figure 4. Integrals of the velocity autocorrelation function for OX, MX, and PX at $T = 298$ K and $P = 0.1$ MPa.

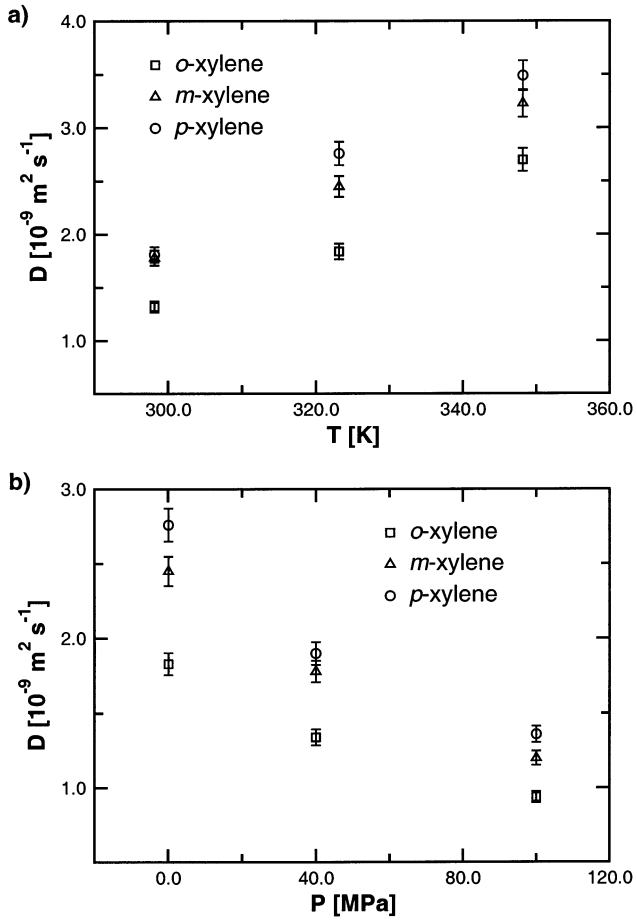

Figure 5. Self-diffusion coefficient vs (a) temperature and (b) pressure for the xylene isomers.

4. Discussion

The availability of viscosity and diffusion data at different pressures and temperatures makes it possible to test the validity of the well-known Stokes−Einstein (SE) equation at the molecular level. In its original form, the SE relation describes the diffusion of a spherical Brownian particle suspended in a liquid. It is obtained by combining the solution of the Langevin equation for the Brownian particle with the solution of the Navier−Stokes equation for the flow around a sphere,

$$D = \frac{k_B T}{C\sigma\eta} \tag{4}$$

TABLE 5: Diffusion Coefficient in [10^{-9} m^2 s^{-1}] for Xylenes at Five State Points[a]

P [MPa]	T [K]	OX	MX	PX
0.1	323.0	1.90	2.46	2.74
40.0	323.0	1.33	1.81	1.98
100.0	323.0	0.94	1.20	1.37
0.1	298.0	1.31	1.73	1.91
0.1	348.0	2.64	3.30	3.60

[a] Statistical errors are less than ±4%.

where η is the viscosity of the surrounding medium, D is the diffusion coefficient of the suspended hard sphere, σ is its diameter, k_B is the Boltzmann constant, and T the temperature of the system. C is a numerical factor which is equal to 6π for stick and 4π for slip boundary conditions. The denominator of the right-hand side represents the drag force of the fluid on the particle.

If the fluid consists of identical spherical molecules, this relationship is generalized by taking each molecule to represent the suspended particle. In this case, the product of the diffusion coefficient and viscosity, divided by temperature, is inversely proportional to some effective diameter of the molecule d_{eff}, i.e., some constant independent of density and (possibly) only weakly dependent on temperature. This generalization of the SE relation has been successfully applied to simple molecular fluids. Jonas and co-workers[20−22] have shown that the SE relation is valid at the molecular level for a variety of fluids with almost spherical (tetramethylsilane) or nonspherical shape (benzene, cyclohexane, methylcyclohexane). For these systems, the effective diameter is constant within 10% over a wide range of densities and temperatures.

We plot in Figure 6 the inverse of the viscosity, $1/\eta$, vs D/k_BT for the xylene isomers for the five considered state points. For each isomer, the data fall on a straight line, meaning that, in the range of temperature and pressure considered here, the SE relation is valid for xylene isomers. This means that all isomers can be represented by hard spheres of some "effective hydrodynamic diameters" d_{eff} independent of state point, whose value is given by the slope of $1/\eta$ vs D/k_BT. Thus, we have

$$\frac{1}{\eta} = d_{eff}\frac{D}{k_B T} \tag{5}$$

which means that xylene isomers in the hydrodynamic limit behave like spherical particles of different size. It is really surprising that such a gross oversimplification works well even for polar molecules which are of quite irregular shape. Recent work from Walser et al.[23] shows that deviations from SE are found for liquid water. The reason for this is that transport in water is strongly influenced by the structure of hydrogen bond network, which in turn depends strongly on temperature. For this reason it is not possible to define an effective diameter of a corresponding spherical particle which would be independent of state point. Therefore, the validity of SE can be extended to nonspherical and polar molecules like xylenes but will fail for hydrogen-bonding liquids like water.

The effective diameters were determined from the slope of a linear least-squares fit of $1/\eta$ vs D/k_BT. For all isomers, the correlation coefficients are better than 0.99, and we find the following values for the effective diameters of xylenes: $d_{OX} = 43.9$ Å, $d_{MX} = 45.9$ Å, and $d_{PX} = 33.4$ Å. As the effective diameter contains averages of several properties (short- and long-range interaction, rotational properties, geometry, etc.), it is expected that different molecules do have different hydrodynamical diameters. However, it is interesting to note that xylene

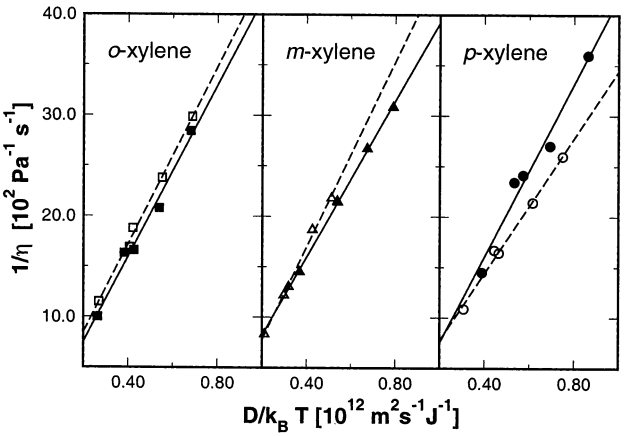

Figure 6. Inverse viscosity vs D/k_BT for charged (open symbol) and not charged (full symbols) xylenes with corresponding linear least-squares fit (charged, dotted line; not charged, full lines). Values of d_{eff} for charged isomers are 43.9, 45.9, and 33.4 Å for OX, MX, and PX, respectively. Values of d_{eff} for not charged isomers are 42.4, 38.7, and 42.7 Å for OX, MX, and PX, respectively.

isomers exhibit quite different values for d_{eff}. It means that the dependence of say D on η is different. Indeed, in our case, we observed what can appear as a counterintuitive result, namely, the order of viscosities of the three isomers at any given state point is different from the order of the inverse self-diffusion coefficient. The following order is observed for viscosities:

$$\eta_{OX} > \eta_{PX} > \eta_{MX}$$

while the order of inverse of self-diffusion is

$$D_{OX}^{-1} > D_{MX}^{-1} > D_{PX}^{-1}$$

For *similar* molecules, i.e., with very close hydrodynamic radii, we would not observe this inversion of transport coefficients.

To determine which property of the potential has as for a consequence the "reversal order" of viscosities, we considered separately the influence of change of shape induced by charges and the way distribution of mass affects the effective molecular diameter.

4.1. Influence of Charges on Shape. To determine how the presence of charges influences the effective diameter in the Stokes−Einstein equation, we set all the site charges to zero and calculate the resulting density and transport properties. The results of simulations without charges at the state point $T =$ 298 K and $P = 0.1$ MPa are shown in Table 6.

When the electrostatic interactions are removed, there is roughly a 1−1.5% decrease in density. This is mostly due to the change in packing structure because of the change of shape. The transport properties change considerably—specifically diffusion coefficient increases and viscosity decreases. This is not only the consequence of the change of density as can be seen from the self-diffusion and viscosity values at the density of charged isomers (see D_{nc}^* and η_{nc}^*, Table 6), because the order of viscosity is now inverse to the order of diffusion coefficients. Indeed, if we calculate the Stokes−Einstein effective diameters, which are independent of density, we find that their order for MX and PX is reversed (Figure 6). There had been some discussion in the literature on whether the transport coefficients change only because of the change in density when electrostatic interactions are included.[24,25] This was shown to hold for Stockmayer fluids,[24] e.g., for acetone, but not for hydrogen-bonding liquids such as water and methanol. It is certainly not true in our case. We consider that the influence of electrostatics cannot be reduced to the change in density in the case of very anisotropic potential. A Stockmayer molecule changes from spherical to slightly ellipsoid, and acetone becomes a little more elongated, but the general properties of the shape are not altered much. In the case of xylene molecules, the LJ potential is highly irregular, and putting 12 charges on LJ sites changes it unpredictably.

4.2. The Role of the Moment of Inertia. The moment of inertia of a molecule determines how fast it would rotate in response to a given torque. Lee and Cummings[24] have investigated the effect of the inertia tensor for polar fluids with uniformly distributed mass, e.g., the Stockmayer fluid. By increasing the diagonal elements of the inertia tensor by a factor of 4, they observed an increase in the viscosity of roughly 10%. For irregularly shaped molecules, like xylene isomers, the three diagonal elements of the inertia tensor give a rate of rotation around each of the principal axes of rotation in response to the same torque. If the shape of a molecule, given by its potential (e.g., in the case of a LJ-type potential, the shape is mostly given by its repulsive part), is elongated in one direction, we intuitively expect that its mass would be distributed in a similar way, so that the moment of inertia around this elongated axis would be smaller than the moment of inertia around the axis perpendicular to it. This means that such a body would rotate faster around an axis which is more elongated. However, one can imagine a situation where the distribution of mass does not match the elongation of the potential (shape). Such a body would, in response to the same torque, rotate faster around an axis along which it is shorter, which would change its transport properties. By determining in which way D and η change when the relationship between mass distribution and potential elongation is reversed, we can deduce in which way charges change the shape of xylene molecules relative to principal axes of rotation.

With this aim, we interchange the x and y diagonal moments of inertia, while leaving the coordinates of force centers unchanged. Such a reversal of axes is simple to perform when a molecule is represented as a rigid body, because the mass sites are not specifically defined, but one assigns the elements of the inertia tensor, and positions of force sites in the system of principal axes, while total mass is assigned as a separate variable.

As equilibrium thermodynamic properties do not depend on mass or inertia tensor, this transformation does not affect density at a given state point. The results of this interchange for isomers with and without charges are presented in Table 7.

TABLE 6: Comparison between Transport Properties of Charged and Not Charged Xylene Isomers[a]

isomer	ρ_{nc} [kg m^{-3}]	D_{nc} [10^{-9} m^2 s^{-1}]	D_{nc}^* [10^{-9} m^2 s^{-1}]	D [10^{-9} m^2 s^{-1}]	η_{nc} [mPa s]	η_{nc}^* [mPa s]	η [mPa s]
OX	865.5	1.87 ± 0.07	1.75 ± 0.06	1.31 ± 0.01	0.490 ± 0.02	0.600 ± 0.03	0.787 ± 0.060
MX	849.3	2.40 ± 0.02	2.21 ± 0.08	1.73 ± 0.05	0.412 ± 0.02	0.515 ± 0.03	0.578 ± 0.015
PX	844.7	2.47 ± 0.04	2.36 ± 0.03	1.91 ± 0.10	0.368 ± 0.02	0.442 ± 0.04	0.609 ± 0.020

[a] ρ_{nc}, D_{nc}, and η_{nc} are respectively density, self-diffusion coefficient, and viscosity of isomers without charges at 298.5 K and 0.1 MPa. ρ_{nc}^*, D_{nc}^*, and η_{nc}^* are the same quantities computed at the density of charged xylenes at 298.15 K and 0.1 MPa.

TABLE 7: Results of Interchanging the Principal Axes of Rotation[a]

isomer	D [10^{-9} m^2 s^{-1}]	D_{inv} [10^{-9} m^2 s^{-1}]	η [mPa s]	η_{inv} [mPa s]
		Without Charges		
OX	1.87	1.86	0.490	0.533
MX	2.40	2.43	0.412	0.415
PX	2.47	2.50	0.368	0.423
		With Charges		
OX	1.31	1.29	0.767	0.869
MX	1.70	1.73	0.532	0.486
PX	1.91	1.95	0.609	0.621

[a] D and η are the transport coefficients; D_{inv} and η_{inv} are the transport coefficients with interchanged axes.

First, we observe that for all isomers, charged or neutral, the inversion of moments of inertia changes the diffusion coefficient by less than 2%, which is within the simulation error bars. From this we can deduce that the hydrodynamic drag (which is proportional to the effective size of the particle and viscosity of the surrounding medium) is insensitive to the mass distribution as long as the trace of the moment of inertia remains constant.

We proceed to determine whether the molecule with matching shape and mass distribution appears effectively bigger or smaller than the molecule with mismatch. This we can determine from the effect of interchange of moment of inertia on viscosity of PX without charges. Its potential is clearly more elongated along *y* axis, and its moment of inertia around this axis is smaller (Figure 1 and Table 2). The interchange of *x* and *y* elements of moments of inertia would therefore cause a mismatch between the radii of gyration and potential elongations corresponding to these axes. Upon exchange of axes, viscosity of PX without charges increases by 15%, which is significant enough to be considered as a real effect. Since the total friction force remains the same, this implies that a molecule with mismatch appears effectively smaller but that a fluid consisting of such molecules is more viscous than a fluid of particles with matching shape and mass distribution.

If the same test is applied to other isomers, we can see that the elongation of OX potential without charges also matches its mass distribution, while the overall shape of MX without charges is approximately disklike and the interchange of the elements of inertia tensor does not change its viscosity.

When charges are placed on LJ sites, the relationship between the potential and mass distribution for OX and PX does not change, and viscosity is still modified in the same way by the interchange of the inertia tensor elements. In the case of MX, its shape becomes more elongated in the *y* direction when charges are present, introducing a mismatch between shape and mass distribution and therefore a change in viscosity. This is consistent with the dipole moments of OX and MX being oriented along the *y* axis.

The above discussion shows that the change of shape relative to the mass distribution induced by charges does not contribute to the inversion of the order of viscosities of MX and PX. In fact, the relationship between shape and mass distribution in the two cases is such that it would preserve this order. However, the charges can change the shape in many different ways; e.g., they can make the average size of a molecule seem smaller or bigger by making it more or less irregular.

5. Conclusion

We have calculated shear viscosity and self-diffusion transport coefficients of xylene isomers using the OPLS set of parameters for substituted benzenes. Comparison with experimental results for density and viscosity shows that these properties can be well reproduced using this potential, and therefore it is assumed that the diffusion coefficients should be also accurate to the same degree. A good agreement was found with Assael correlation for viscosity data.[13] This correlation has been successfully applied to a wide variety of molecular fluids.[26] It is worth noting here that MD results for self-diffusion could serve as a basis for the evaluation of the rough hard-sphere parameters ("roughness factor" and the "effective" size of the molecule) for xylene isomers for which self-diffusion experimental data are actually missing.

The good agreement between simulation and experimental results is due only to the force field used in simulation. Given the way the potential had been constructed, this agreement is quite amazing. In light of the discussion at the beginning of section 2, it is possible that the ability to reproduce both densities and viscosities is a fortuitous consequence of some cancellation effects in the simple model used.

The accuracy of the simulation results for viscosity (5% error bars) is related to the length of the EMD runs. It is possible that the error bars could have been smaller had we used the NEMD method. However, a discussion of the relative merits of EMD and NEMD is outside the scope of this work.

Using our viscosity and self-diffusion data, we found that xylene isomers do satisfy the SE relationship for a large range of temperatures and pressures. It was shown that, although xylene isomers may seem very similar, they have quite different effective sizes such that, for each studied state, the inverse of the diffusion coefficient of the isomers is not in the same order as viscosities. Some MD simulations at a single state point ($T = 298$ K and $P = 0.1$ MPa) were conducted in order to evaluate the influence of the electrostatic interactions and the mass distribution on the transport properties of xylenes.

When electrostatic interactions are removed, we observe a small decrease in the density at constant P but transport properties change significantly; specifically, diffusion coefficient increases and viscosity decreases. Contrary to the Stockmayer fluid, the change in transport properties is mostly caused by the change of "shape" of xylene isomers with and without charges rather than by the change in density.

With charges, the shape of OX and PX becomes more elongated along the axis with the smallest radius of gyration, whereas MX changes from disklike shape to the one more stretched along the axis with larger moment of inertia. This effect contributes toward preserving the intuitive order of diffusion coefficients and viscosities rather than violating it. The change of shape and effective size because of charges, which causes the inversion of order of viscosities of MX and PX, is not related to mass distribution. However, the influence of rotational properties, or more specifically of the moment of inertia tensor on transport of nonspherical molecules, is worth a more systematic study.

Acknowledgment. J.P. gratefully acknowledges a generous grant of computer time from the Australian Partnership for Advanced Computing National Facility. B.R. thanks Professor Denis J. Evans for hosting his visit to the Research School of Chemistry at A.N.U.

References and Notes

(1) Jorgensen, W. L.; Nguyen, T. B. Monte Carlo simulations of the hydration of substituted benzenes with OPLS potential functions. *J. Comput. Chem.* **1993**, *14*, 195−205.

(2) Jorgensen, W. L.; Severance, D. L. Aromatic−aromatic interactions: Free energy profiles for the benzene dimer in water, chloroform and liquid benzene. *J. Am. Chem. Soc.* **1990**, *112*, 4768−4774.

(3) Rowley, R. L.; Ely, J. F. Non-equilibrium molecular dynamics simulations of structured molecules. II. Isomeric effects on the viscosity of models for *n*-hexane, cyclohexane and benzene. *Mol. Phys.* **1992**, *75*, 713−730.

(4) Karlström, G.; Linse, P.; Wallqvist, A.; Jönsson, B. Intermolecular potentials for the $H_2O-C_6H_6$ and the $C_6H_6-C_6H_6$ systems calculated in an ab initio SCF CI approximation. *J. Am. Chem. Soc.* **1983**, *105*, 3777−3782.

(5) Jorgensen, W. L.; Swenson, C. J. Optimized intermolecular potential functions for amides and peptides. Structure and properties of liquid amides. *J. Am. Chem. Soc.* **1984**, *107*, 569−578.

(6) Jorgensen, W. L. Intermolecular potential functions and Monte Carlo simulations for liquid sulfur compounds. *J. Phys. Chem.* **1986**, *90*, 6379−6388.

(7) Briggs, J. M.; Matsui, T.; Jorgensen, W. L. Monte Carlo simulations of Liquid alkyl ethers with the OPLS potential Functions. *J. Comput. Chem.* **1990**, *11*, 958−971.

(8) Jorgensen, W. L.; Laird, E. R.; Nguyen, T. B.; Tirado-Rives, J. Monte Carlo simulations of pure liquid substituted benzenes with OPLS potential functions. *J. Comput. Chem.* **1993**, *14*, 206−215.

(9) Verlet, L. Computer 'experiments' on classical fluids. I. Thermodynamical properties of Lennard-Jones molecules. *Phys. Rev.* **1967**, *159*, 98−103.

(10) Nosé, S.; Klein, M. L. Constante pressure dynamics for molecular systems. *Mol. Phys.* **1983**, *50*, 1055−1076.

(11) Evans, D. J.; Morriss, G. P. *Statistical Mechanics of Nonequilibrium liquids*; Academic Press: London, 1990.

(12) Evans, D. J. On the representation of orientation in space. *Mol. Phys.* **1977**, *34*, 317−325.

(13) Assael, M. J.; Dymond, J. H.; Patterson, P. M. Correlation and prediction of dense fluid transport coefficients. V. Aromatic hydrocarbons. *Int. J. Thermophys.* **1992**, *13*, 895−905.

(14) Kashiwagi, H.; Makita, T. Viscosity of twelve hydrocarbon liquids in the temperature range 298−348 K at pressures up to 110 MPa. *Int. J. Thermophys.* **1982**, *3*, 289−305.

(15) Dymond, J. H.; Robertson, J. Transport properties of nonelectrolyte liquid mixture. VI. Viscometric study of binary mixtures of hexafluorobenzene with aromatic hydrocarbons. *Int. J. Thermophys.* **1985**, *6*, 21−41.

(16) Assael, M. J.; Papadaki, M.; Wakeham, W. A. Measurements of the viscosity of benzene, toluene and *m*-xylene at pressure up to 80 MPa. *Int. J. Thermophys.* **1991**, *12*, 449−457.

(17) Et-Tahir, A. Détermination des variations de la viscosité de divers hydrocarbures en fonction de la pression et de la température. Etude critique de modèles représentatifs. Thèse de Doctorat, Université de Pau et des Pays de l'Adour, 1993.

(18) Wick, C. D.; Martin, M. G.; Siepmann, J. I. Transferable potentials for phase equilibria. 4. United atom description of linear and branched alkenes and alkylbenzenes. *J. Phys. Chem. B* **2000**, *104*, 8008−8016.

(19) Daivis, P. J.; Evans, D. J. Comparison of constant pressure and constant volume nonequilibrium simulations of sheared model decane. *J. Chem. Phys.* **1994**, *100*, 541−547.

(20) Parkhurst, H. J.; Jonas, J. Dense liquids. II. The effect of density and temperature on viscosity of tetramethylsilane and benzene. *J. Chem. Phys.* **1975**, *63*, 2705−2709.

(21) Jonas, J. D.; Huang, S. G. Self-diffusion and viscosity of methylcyclohexane in the dense liquid region. *J. Chem. Phys.* **1979**, *71*, 3996−4000.

(22) Jonas, J.; Hasha, D.; Huang, S. G. Density effect on transport properties in liquid cyclohexane. *J. Phys. Chem.* **1980**, *84*, 109−112.

(23) Walser, R.; Hess, B.; Mark, A. E.; van Gunsteren, W. F. Further investigation on the validity of Stokes−Einstein behaviour at the molecular level. *Chem. Phys. Lett.* **2001**, *334*, 337−342.

(24) Lee, S. H.; Cummings, P. T. Shear viscosity of model mixtures by nonequilibrium molecular dynamics. II. Effect of dipolar interactions. *J. Chem. Phys.* **1996**, *105*, 2044−2055.

(25) Wheeler, D. R.; Rowley, R. L. Shear viscosity of polar liquid mixtures via nonequilibrium molecular dynamics: Water, methanol, and acetone. *Mol. Phys.* **1998**, *94*, 555−564.

(26) Assael, M. J.; Truesler, J. P. M.; Tsolakis, T. F. *Thermophysical Properties of Fluids−An introduction to their prediction*; Imperial College Press: London, 1996.